Variable restriction of albumin diffusion across inflamed cerebral microvessels of the anaesthetized rat

A. S. Easton and P. A. Fraser

Vascular Biology Research Centre Physiology Group, Biomedical Sciences Division, King's College London, Campden Hill Road, London W8 7AH

1. The possibility of restricted diffusion of macromolecules in single cerebral venular capillaries that have become leaky due to inflammation was investigated by comparing the permeabilities to Lucifer Yellow (457 Da; P_{LY}) and rhodamine-labelled albumin (69 kDa; $P_{Rh\text{-}A}$).

2. The dyes were trapped between two micro-occlusion probes and the permeabilities were measured from the rates of decrease in dye fluorescence at low intraluminal hydrostatic pressure.

3. Removal of one probe had little effect on P_{LY} but did reduce $P_{Rh\text{-}A}$, consistent with the influence of convection on diffusion through 22 nm wide transendothelial slits 1 μm deep.

4. Direct comparisons were made over time between P_{LY} and $P_{Rh\text{-}A}$ in six vessels while hydrostatic pressure effects were controlled. In all vessels $P_{Rh\text{-}A}:P_{LY}$ varied from being similar to the ratio of the free diffusion coefficients to virtually zero even though P_{LY} remained high. The question of the source of this variable restriction to albumin is discussed in terms of the secretion and sloughing of glycosaminoglycans and the possible role of transient formation of transendothelial gaps.

The very low permeability of the cerebral microcirculation to polar solutes and macromolecules is often referred to as the blood–brain barrier (BBB). This barrier may be disrupted in a number of pathological states such as cerebrovascular accident, epilepsy, multiple sclerosis and cerebral neoplasia, and increased permeability to plasma proteins is a key factor in the subsequent development of cerebral oedema. Experimental disruption of the barrier has been induced in a variety of ways, such as hyperosmotic solutions (Rapoport, 1970), acute hypertension (Byrom, 1954; Johansson, Li, Olsson & Klatzo, 1970), high inhaled CO_2 (Clemedson, Hartelius & Holmberg, 1958), repeated seizures (Bjerner, Broman & Swensson, 1944), radiation damage (Clemente & Holst, 1954), middle cerebral artery occlusion (Tamura, Graham, McCulloch & Teasdale, 1981) and simple exposure following craniotomy (Edvinnson & West, 1972).

Most evidence suggests that blood–brain barrier disruption occurs as a result of the opening of the extremely tight junctions between neighbouring endothelial cells. Both Robinson & Rapoport (1987) and Fraser & Dallas (1990) have calculated that the osmotically opened barrier is best explained as 22 nm wide parallel-sided slits between endothelial cells. This is consistent with the independently measured mean cleft width of 22 nm in single frog mesenteric vessels (Clough & Michel, 1988) which have a similar permeability to small hydrophilic molecules as disrupted frog pial microvessels (Fraser & Dallas, 1993). There is evidence that hydrostatic pressure drives a bulk flow through the same pathway as that through which the molecules diffuse in systemic capillaries (Curry, Joyner & Rutledge, 1990) and in leaky cerebral capillaries of the frog (Fraser & Dallas, 1993). This has important consequences for the measurement of permeability, which should be more apparent for larger molecules. We tested this by altering the intracapillary hydrostatic pressure during measurements of permeability.

The aim of the experiments described here was to characterize the permeability of pial microvessels of the rat, which had become leaky following removal of the skull and overlying meninges, to a protein and a hydrophilic low molecular weight dye. The permeabilities to Lucifer Yellow and rhodamine-labelled albumin were measured using a modification of the single microvessel occlusion technique in which it was also possible to examine effects due to changes in hydrostatic pressure.

A brief description of some of these experiments has been published previously (Easton & Fraser, 1991).

METHODS

Measurements and data handling

Intracarotid injections of Lucifer Yellow or rhodamine-labelled albumin were given in repeated boluses of between 0·05 and 0·2 ml. As the dye passed through the microcirculation it was trapped in a venular segment 200–300 μm in length by lowering a glass occluding probe onto the microvessel. A second occluding probe could be placed 100–200 μm away from the first probe to generate a segment of microvessel in which hydrostatic pressure would fall in time. The calculation in the Appendix shows that

List of symbols

Symbol	Definition	Units
σ	Reflection coefficient	—
A_p	Area of porous pathway per unit area of endothelium	—
Δx	Endothelial cleft depth	cm
C	Normalized concentration of dye	—
D	Free diffusion coefficient	$cm^2\ s^{-1}$
J_v	Volume flux per unit area	$cm\ s^{-1}$
L_p	Hydraulic conductance	$cm\ cmH_2O^{-1}\ s^{-1}$
P_0	Diffusive permeability coefficient ($DA_p/\Delta x$)	$cm\ s^{-1}$
P_s	Combined convective and diffusive permeability coefficient ($P_0 Z + J_v(1-\sigma)$)	$cm\ s^{-1}$
P'	Experimental permeability ($P_s - J_v$)	$cm\ s^{-1}$
Pe	Péclet number ($J_v(1-\sigma)/P_0$)	—
r	Radius of occluded segment	cm
Z	$Pe/(e^{Pe}-1)$	—

the intraluminal pressure should fall to 2·5 % of the initial value within 1 min.

The diagram below (Fig. 1) illustrates the experimental condition of an occluded vessel filled with dye. Measurements of dye concentration were made from a vessel section close to the occluding probe, but not so close that the vessel geometry was distorted.

The approach that underlies this work was fully detailed previously (Fraser & Dallas, 1990, 1993) and the following is a brief account. At early times in a singly occluded vessel, that is while the axial dye concentration is uniform along the measured segment, with a dye concentration outside the vessel of zero, dye concentration will fall according to

$$C_t = C_0 e^{-kt}, \tag{1}$$

with

$$k = \frac{2}{r} P'. \tag{2}$$

P' is an experimentally derived permeability coefficient, which is related to the convective and combined convective and diffusive permeability coefficients by

$$P' = P_s - J_v = P_0 Z + J_v(1-\sigma) - J_v, \tag{3}$$

from which

$$\frac{P'}{P_0} = Z + \mathrm{Pe} - \frac{J_v}{P_0} = Z - \frac{J_v \sigma}{P_0}, \tag{4}$$

where Pe, the Péclet number, is the ratio of the convective to the diffusive velocities through a channel shared by solute and solvent, and Z is the ratio by which the concentration gradient that drives diffusion ($\Delta C/\Delta x$) is reduced by the velocity of fluid flow through the porous pathway. When σ is small the parameter Z approximates to the ratio P'/P_0. P' will be a good estimate for P_0 when Pe is small. These equations were combined with those derived from the hydrodynamic pore theory (Curry 1974, 1984; which give permeability, filtration and reflection coefficients in terms of parallel-sided slit width), to obtain a plot of theoretical P'/P_0 profiles for differing slit widths and hydrostatic pressures for Lucifer Yellow (LY: 457 Da) and for rhodamine–albumin (Rh-A: 69 kDa) (Fig. 2). These graphs demonstrate that at slit widths of less than 30 nm P'_{LY} is relatively insensitive to hydrostatic pressure, whereas $P'_{Rh\text{-}A}$ would be expected to fall rapidly as pressure is increased. With two occluding probes applied to the microvessel, the hydrostatic pressure within the segment will fall to very low values after a minute or so (see Appendix). In this condition the measured permeability P' will be close to the diffusive permeability P_0, and by lifting one probe and restoring the hydrostatic pressure it is possible to estimate P' and P_0 in the same vessel.

Animal preparation

Experiments were performed on Wistar rats aged between 23 and 33 days. Anaesthesia was induced by intraperitoneal injection of 0·72 ml kg^{-1} urethane (25 % w/v in 0·9 % NaCl solution) and maintained where necessary with intravenous doses of 0·08 ml kg^{-1}. All rats were pretreated with 1 mg dexamethasone, 2 mg indomethacin, 10 mg cimetidine and 1 mg mepyramine by intraperitoneal injection. A thermal probe was inserted rectally and the animal maintained at 37 ± 1 °C using a heating blanket connected via the probe to a feedback circuit (CFP 8105 Harvard Instruments, Edenbridge, UK). Orthograde cannulation of the left common carotid artery was carried out routinely.

A section of the frontoparietal bones on the left side, approximately 5 × 5 mm between the coronal and lamboid sutures, was thinned with a dental drill and removed. Great care was taken to avoid trauma to the mid-line sagittal or the inferior transverse venous sinuses. The cerebral surface was exposed by cutting away the overlying meninges, which in these young rats leaves the pial microvessels devoid of any continuous layer of overlying tissue (Butt, Jones & Abbott, 1990). The rat was then placed on the modified stage of a microscope (ACM, Zeiss, Oberkocken, Germany) and illuminated with a 50 W mercury vapour lamp through a ×20 objective lens (Cooke, NA 0·5) fitted with a water immersion cap to eliminate the air–water meniscus. The surface of the brain was constantly superfused at the rate of 1–2 ml min^{-1} with artificial cerebrospinal fluid (ACSF) delivered through a fine plastic tube attached to the side of the water immersion cap. The superfusate was warmed to 37 ± 1 °C. The occluding probes were made from borosilicate glass tubes (outside diameter 1 mm; Clark Electromedical, Pangbourne, UK; drawn and sealed to produce a rounded tip *ca* 20 μm) and placed in a Leitz micromanipulator positioned on the microscope stage.

The instrumentation was very similar to that fully described by Fraser & Dallas (1990). The microscope image was led to an image-intensifier camera (Panasonic WV-1900, Japan). The raw camera signal was monitored directly on an oscilloscope (Hitatchi V202-F, Japan) and led to a video-timer (For-A,

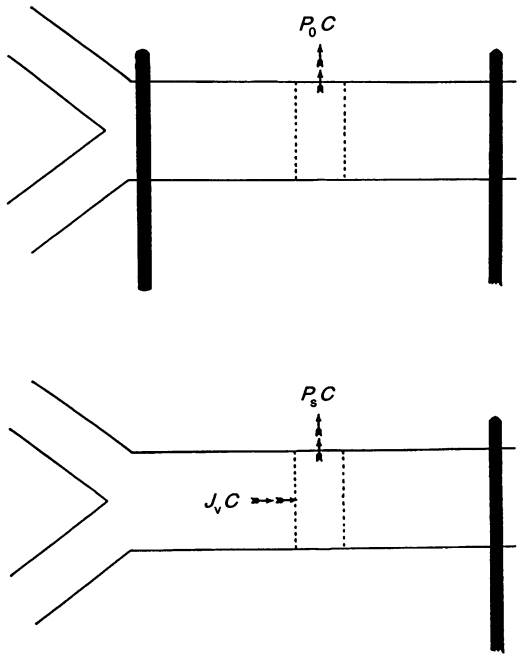

Figure 1. Schematic diagrams showing the arrangement of the microvessels and the microneedles in the double- and single-occlusion experiments
The dye concentration was measured from the area outlined by the dotted lines.

Japan) through a video-densitometer and television monitor (Electrohome EMV-1710R(X), Canada). The output of the video-densitometer was taken to a chart recorder (Lectromed M19, Welwyn Garden City, UK). The video-densitometer operated by integrating the video signal between variable electronic gates used to create a bright cursor on the television monitor. The cursor was placed over a segment of the vessel close to (approximately 100 μm) from the downstream occluding probe, but not so close as to suffer from geometric distortion. The light signal due to trapped dye was proportional to its concentration (Fraser & Dallas, 1990) and was relayed by the video-densitometer during experiments directly to the chart recorder. Light in the interstitium near the vessel was measured for each occlusion and subtracted from the measurements. Capillary diameters were

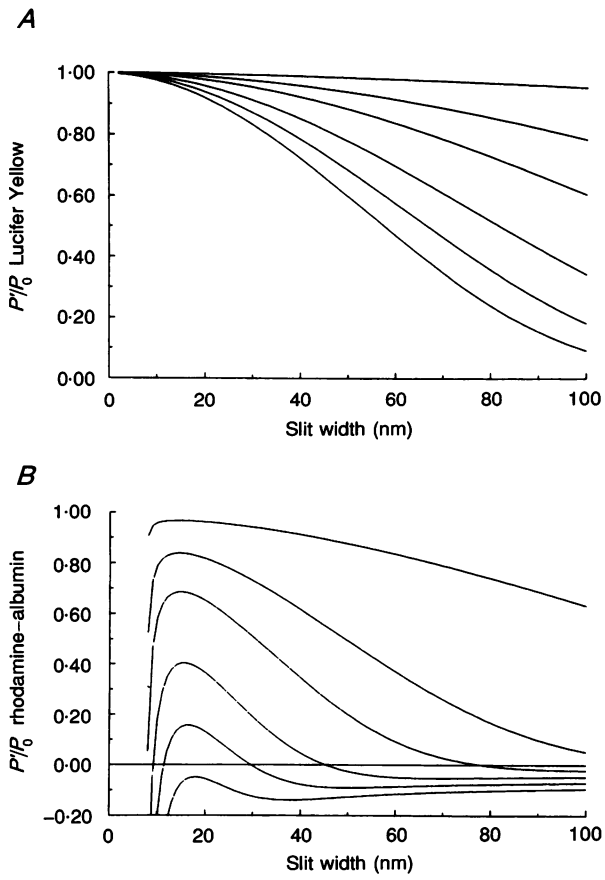

Figure 2. Changes in P' with slit width for different hydrostatic pressures
Plots, based on eqn (4) and pore theory equations modified for slits (Curry, 1984), showing how the experimental permeability is thought to decrease as a fraction of the true diffusional permeability as slit width and transmural hydrostatic pressure increase. The diagrams (*A*, Lucifer Yellow; *B*, rhodamine–albumin) give P'/P_0 for pressures of 1, 5, 10, 20, 30 and 40 cmH_2O from top to bottom.

measured directly from the television monitor which had been calibrated previously for the microscope using a stage micrometer. The geometry of the microvessels was assessed by capturing images of occluded vessels in an image processor (DIS 3000; Digital Imaging Systems, Newport, Gwent) and measuring the fluorescence intensity across the diameter. The rate of fading of both dyes was insignificant for the occlusion durations and illuminating intensities used, amounting to no more than 10 % of the rate of decline in the light signal for the slowest rates of dye loss observed.

Solutions

ACSF was buffered to pH 7·4 ± 0·5 and contained (mM): NaCl, 110·5; KCl, 4·7; $CaCl_2$, 1·25; KH_2PO_4, 1·1; $MgSO_4.7H_2O$, 1·25; $NaHCO_3$, 25; and Hepes, 15. Lucifer Yellow (5 mM, Sigma, St Louis, MO, USA) was made up in 0·9 % NaCl solution. Rhodamine–albumin (2 %) in 0·9 % NaCl was the kind donation of Dr Peter Weinburg of Imperial College, London. Facilities for purification of rhodamine–albumin including sodium dodecyl sulphate-gel chromatography and freeze drying were kindly provided by Pfizer Central Research, Sandwich, Kent.

RESULTS

The autofluorescence of the exposed cerebral surface was sufficient (when illuminated through a fluorescein filter set) for it to be viewed directly under the microscope. Networks of vessels were seen with main vessels running away from the mid-line and smaller branches leaving at various angles. Arteries and arterioles were long and straight with fewer branches than the venular capillaries, which were shorter and more tortuous. A venular capillary with a straight unbranching section of at least 200 μm was selected and the glass occluding probe positioned at one end of the vessel, furthest downstream to the flow. A bolus of fluorescent dye-containing solution was then injected through the carotid arterial cannula, and during its transit through the microcirculation the arterioles filled rapidly followed by a slower venular filling. This was also used to help distinguish venular capillaries from arterioles and the glass occluding probe lowered onto the venular capillary to trap the dye. Initially, at times shortly after the exposure of the cerebral

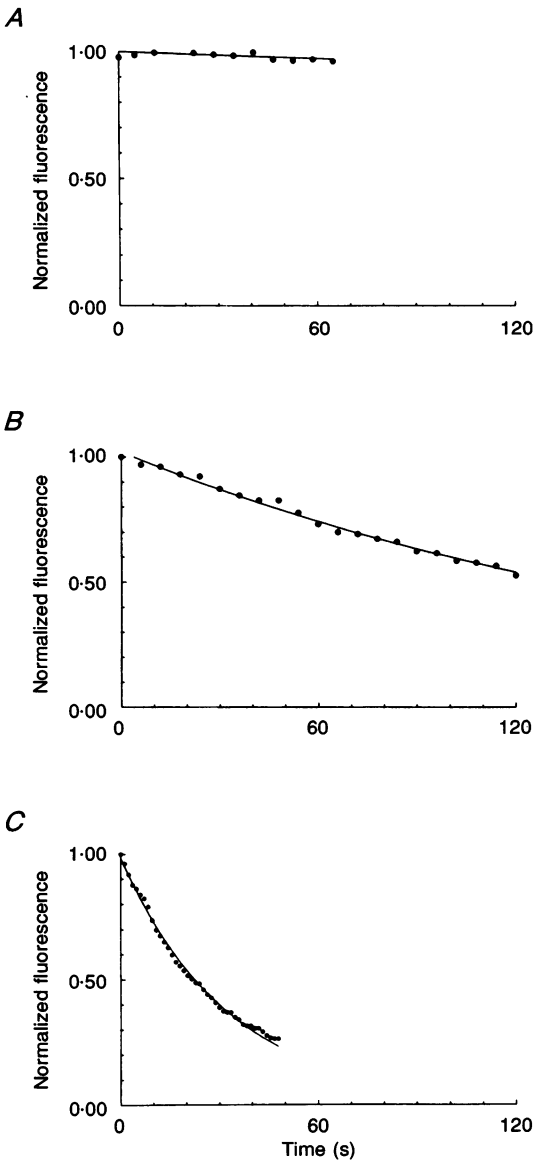

Figure 3. Lucifer Yellow concentration plotted against time in three occlusions from the same venular capillary at 10 (*A*), 30 (*B*) and 60 min (*C*) after exteriorization
These records show the progressive disruption of the vessel from blood–brain barrier to one with a permeability similar to a skeletal muscle capillary.

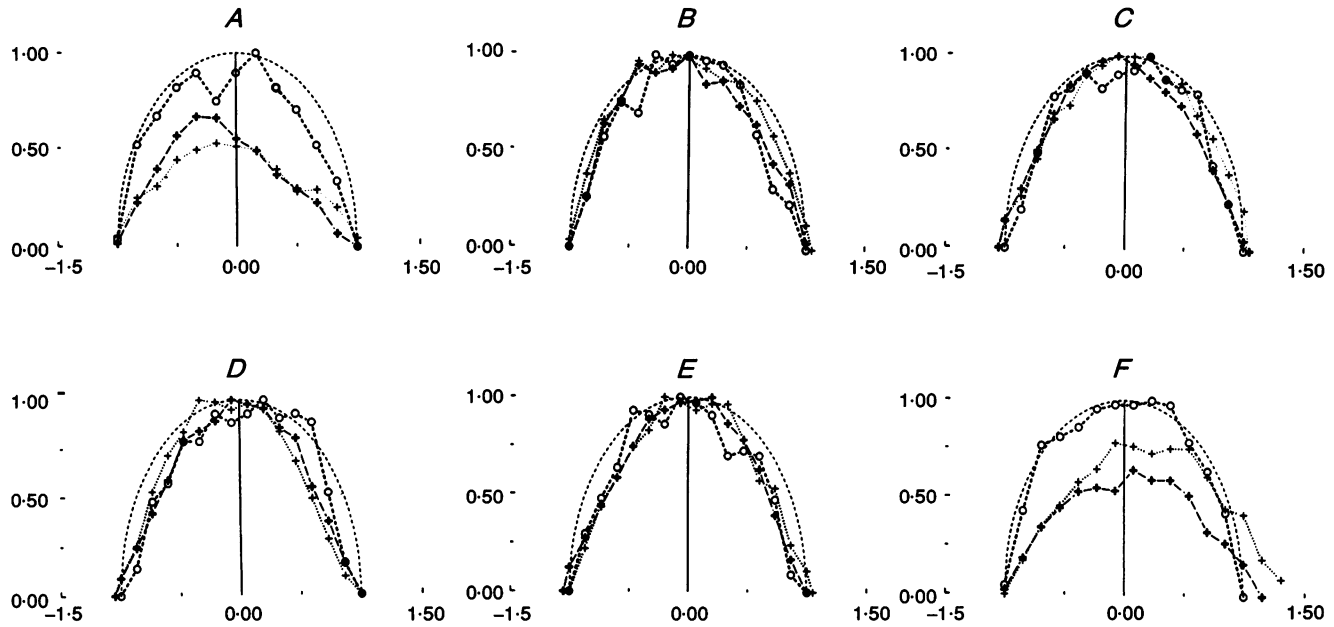

Figure 4. Estimate of the shape of a doubly occluded venular capillary segment (as illustrated in upper diagram in Fig. 1)

The fluorescence intensity (vertical scale) was plotted against the fractional radial distance (horizontal scale) from the centre of the same microvessel at three times (○, before occlusion; +, 60 s and +, 120 s after occlusion started) at different sites (*A–F*) along the segment. The intensity was normalized to the peak value obtained at the relevant time. Site *A* was 14 μm from the mid-point of the left occluding probe; *B*, 28; *C*, 42; *D*, 49; *E*, 63; and *F*, 70 μm. *F* was also 5 μm from the right probe. The dashed line with no symbols represents the fluorescence expected from a perfect cylinder.

surface, there was virtually no dye loss from an occluded segment, which corresponds to an intact blood–brain barrier. After 10–20 min dye loss was measurable, but slow, and at about 1 h there was a marked increase in permeability, which is consistent with inflammation and may be described as a second stage of permeability increase (Easton & Fraser, 1992*a*). Figure 3 illustrates the progressive changes in P'_{LY} in one such venular capillary, and the remainder of this study

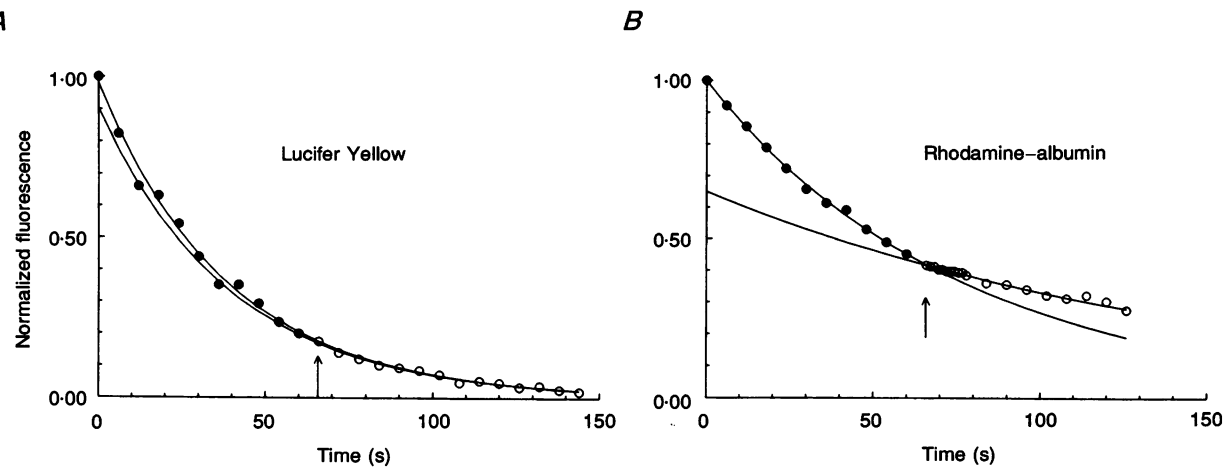

Figure 5. The effect of hydrostatic pressure on rate of decrease of dye concentration in a 14 μm diameter venular capillary

Dye concentration measurements were started about 1 min after the second occluding probe was applied (●). The normal vessel hydrostatic pressure was restored after a further minute (arrow and ○) by raising one of the occluding probes. The rate constant for the fall in Lucifer Yellow concentration was only slightly reduced by the increased pressure (*A*), while that of rhodamine–albumin was halved (*B*).

Table 1. Transendothelial volume flux

Diameter (cm × 10^4)	$\delta C/\delta t_0$ (s^{-1})	J_v (cm × 10^6)	P_{LY} (cm × 10^6)	Pe
24	0·0047	2·34	10·2	0·223
14	0·0100	3·51	14·0	0·243
19	0·0040	1·88	45·3	0·040
28	0·0053	3·71	36·6	0·098
26	0·0088	5·72	25·4	0·219
26	0·0109	7·09	39·5	0·174
Mean		4·09	28·5	0·166
S.E.M.		0·751	5·332	0·0329

Volume fluxes for 6 occlusions on 5 cerebral venular capillaries when $P_{Rh\text{-}A} \approx 0$ and the values for P_{LY} obtained from the same vessels within 1 min of each other.

is concerned with vessels in this high phase of permeability.

Once a leaky vessel had been located a second occluding probe was positioned at its opposite end to allow double occlusions to be performed. Dye escaping from the occluded vessels was washed away by the superfusing solution and was not observed in the surrounding tissues. It is important to know that the geometry of the microvessel does not change significantly during an occlusion, and this was checked by measuring the fluorescence intensity of images of an occluded segment that were captured in the image processor before and during a double-occlusion experiment. Figure 4 shows that the shape is constant and approximately circular throughout the period of occlusion provided that measurements were made at least 30 μm away from the probe.

Effects of single and double occlusions on experimental permeability

The idea that convection plays a significant role in the transfer of large molecules but not small ones was tested by changing the hydrostatic pressure during an occlusion experiment. The dye was trapped between two occluding probes. The fluorescence changes during the first minute while the intraluminal hydrostatic pressure was dissipated were ignored. The permeability measurement was carried out during the next 30–60 s, after which one probe was raised to restore normal hydrostatic pressure to the vessel.

Figure 5*A* shows the effect of double and single occlusions performed sequentially on a vessel containing Lucifer Yellow and shows that there was little change in the rate of dye loss. Similar experiments were carried out with rhodamine–albumin, and Fig. 5*B* shows a typical result: raising one needle was followed by a lower rate of fall in fluorescence. All occlusions with rhodamine–albumin that had an appreciable rate of decrease in fluorescence during a double occlusion showed a reduced rate of loss during the sequential single occlusion. Figure 6 illustrates the relationship between double- and single-occlusion measurements for the two molecules in a total of twelve venular capillaries. The ratio of single- to double-occlusion values (estimated from the regression) in Fig. 6 of P'_{LY} was $0{\cdot}940 \pm 0{\cdot}015$ (mean ± S.E.M., $n = 6$) and a paired t test confirmed that this small decrease was significant (one tail, $P < 0{\cdot}025$), while the ratio of single- to double-occlusion values of $P'_{Rh\text{-}A}$ was $0{\cdot}505 \pm 0{\cdot}056$ ($n = 6$; $P < 0{\cdot}01$). In subsequent experiments single-occlusion measurements were used to estimate P_0 for Lucifer Yellow (P_{LY}) and double-occlusion measurements for rhodamine–albumin P_0 ($P_{Rh\text{-}A}$).

Estimates of P_{LY} and $P_{Rh\text{-}A}$ in the same microvessel

P_{LY} and $P_{Rh\text{-}A}$ were estimated at frequent intervals on six cerebral venular capillaries (diameter range 18–28 μm) over 3·5 h after exposing the brain surface and Fig. 7 shows these

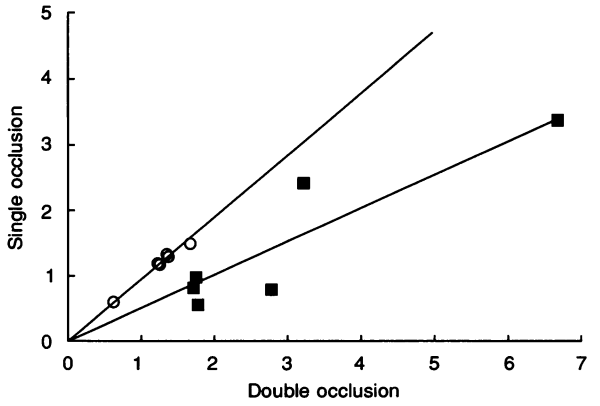

Figure 6. Paired single- and double-occlusion measurements of permeability to Lucifer Yellow (○; cm s^{-1} × 10^5) and rhodamine–albumin (■; cm s^{-1} × 10^6) from 12 different venular capillaries

The gradient of regression through the Lucifer Yellow points is $0{\cdot}940 \pm 0{\cdot}015$, while that through the rhodamine–albumin points is $0{\cdot}505 \pm 0{\cdot}056$.

results. The mean values obtained from all the occlusions for P_{LY} and $P_{Rh\text{-}A}$ were $31{\cdot}6 \pm 1{\cdot}87 \times 10^{-6}$ cm s^{-1} ($n = 56$) and $1{\cdot}28 \pm 0{\cdot}479 \times 10^{-6}$ cm s^{-1} ($n = 97$) respectively. On a number of occasions $P_{Rh\text{-}A}$ was close to the value predicted from P_{LY} and the estimated ratio of the free diffusion coefficients, $D_{Rh\text{-}A}/D_{LY} = 0{\cdot}139$, and shows that at these times there is little restriction to albumin. At other times the value of $P_{Rh\text{-}A}$ was considerably below that expected, and gives clear evidence of restriction. The variability in the measurements of $P_{Rh\text{-}A}$ (coefficient of variation $= 1{\cdot}188 \pm 0{\cdot}0682$, $n = 6$) was much greater than that for P_{LY} ($0{\cdot}428 \pm 0{\cdot}0555$, $n = 6$), as would be expected. There was no apparent pattern in time when albumin would diffuse freely or be restricted.

Estimates of solvent flux

The rate of rhodamine–albumin leakage varied considerably and on some occasions $P_{Rh\text{-}A}$ was immeasurably small (any value less than $0{\cdot}2 \times 10^{-6}$ cm s^{-1} is below the resolution of the method; note size of error bars in Fig. 7) even though P_{LY} remained high. When such a very low $P_{Rh\text{-}A}$ was found with a double occlusion, the upstream occluding probe was raised to restore the hydrostatic pressure. On each occasion

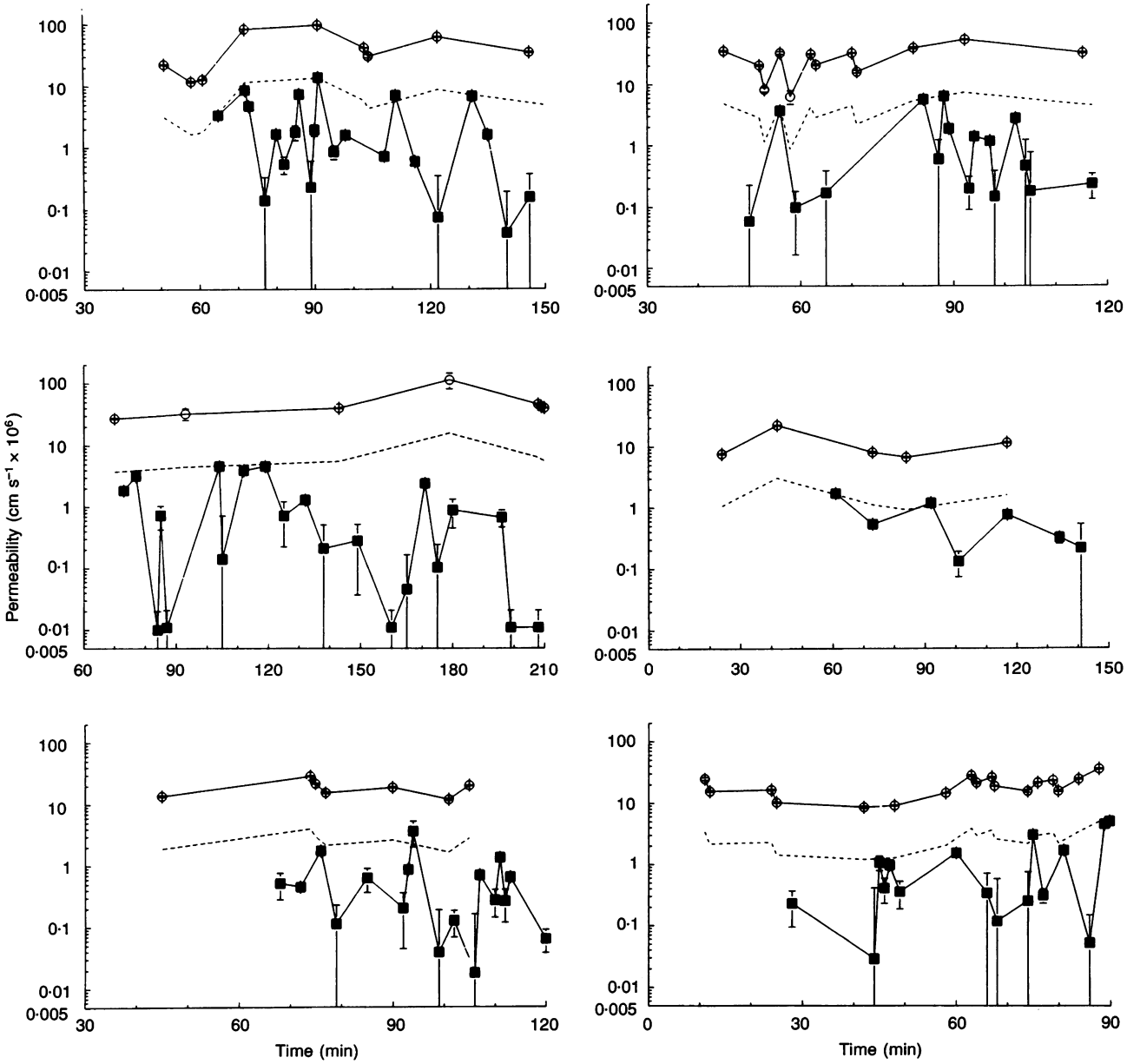

Figure 7. Measurements of P_{LY} and $P_{Rh\text{-}A}$ made on 6 venular capillaries over 1–3 h
The upper points (○) refer to Lucifer Yellow and the lower ones (■) to rhodamine–albumin permeabilities (cm s^{-1} x 10^6). The dashed lines were derived from $P_{LY} \times D_{Rh\text{-}A}/D_{LY}$ and thus represent the predicted permeability to albumin assuming no restriction. The error bars falling below $0{\cdot}2 \times 10^{-6}$ are indications that these permeabilities were below the resolution of the method.

the rhodamine–albumin fluorescence rose with time, as if these vessels were behaving as normal peripheral microvessels (see Fig. 8). The rate of increase in dye concentration ($\delta C/\delta t$) slowed in time, presumably as a consequence of increasing protein concentration polarization across the endothelium and the rising osmotic pressure opposing the luminal hydrostatic pressure. These concentrating occlusions were used to calculate the trans-endothelial volume flux per unit area (J_v) from

$$J_v C_0 = \frac{r}{2}\frac{\delta C}{\delta t_0}. \quad (5)$$

This calculation depends on no dye being lost across the vessel wall as well as the dye concentration along the length of the segment being uniform in the region of the measured section. Table 1 gives these calculated values for six occlusions from five vessels with the values for P_{LY} taken from adjacent occlusions.

It is possible to calculate the Péclet number for Lucifer Yellow from P_{LY} measurements and the estimates of volume flux (obtained from single occlusion pairs of the double occlusions in which rhodamine–albumin did not leak) taken at about the same time. The reflection coefficient to Lucifer Yellow (σ_{LY}) was estimated by assuming that albumin was just retained (i.e. $P_{Rh\text{-}A} \leqslant 0{\cdot}2 \times 10^{-6}$ cm s^{-1}) in the microvessel by a fibre matrix of secreted glycosaminoglycans (GAGs), with fibre radius of 0·6 nm (basic equations given in Curry, 1984). This gave a void volume of 0·963, not too far from the values used in interstitial and endothelial fibre matrix calculations by Curry & Huxley (1982) and gave $\sigma_{LY} = 0{\cdot}029$. The values obtained for Pe_{LY} are also shown in Table 1.

DISCUSSION

These experiments show that the transport of albumin across the disrupted blood–brain barrier is subject to a variation that is not explicable by changes in hydrostatic pressure alone. The implication that this finding has for the nature of the porous pathway in these microvessels will be discussed below, but first some of the tacit assumptions of the method will be considered.

The analysis depends on a uniform dye concentration along the microvessel axis, and two separate processes that occur during an occlusion may be expected to distort this distribution. Fresh fluid, free of dye, drawn into the vessel to replace that lost across the endothelium, would eventually result in the dilution of dye in the measured section. At the same time dye would be expected to diffuse axially to the dye-free region. If these effects were important, the rate of fall of fluorescence would be expected to increase with time. The use of a second occluding probe placed at the entrance of the vessel should eliminate any axial convection, but despite this we saw little difference in P_{LY} measurements between single and double occlusions. This indicates that, in the first minute of an occlusion, axial convection effects are not significant. If such effects were significant in the rhodamine–albumin experiments, the rate of fall of fluorescence should be greater with single compared with double occlusions, whereas the reverse was observed.

Increases in rate of dye disappearance could also represent an incomplete occlusion, but slippage resulted in an obvious appearance of dye flowing past the occluding probe or movement of blood cells trapped within the segment and resulted in a clear increase in the rate of loss of dye from the area of measurement. Undetected leaks past the occluding probe may have resulted in a small increase in the rate of fluorescence decrease, but would not significantly affect the measured values (see Fraser & Dallas, 1993).

The lack of any diffusional barrier between the surface of the exposed pial microvessels and the superfusing solution is another important assumption. Butt *et al.* (1990) showed that ionic lanthanum penetrated to the pial vessels when superfused over similar preparations, so it seems likely that no continuous barrier remains. This concurs with our

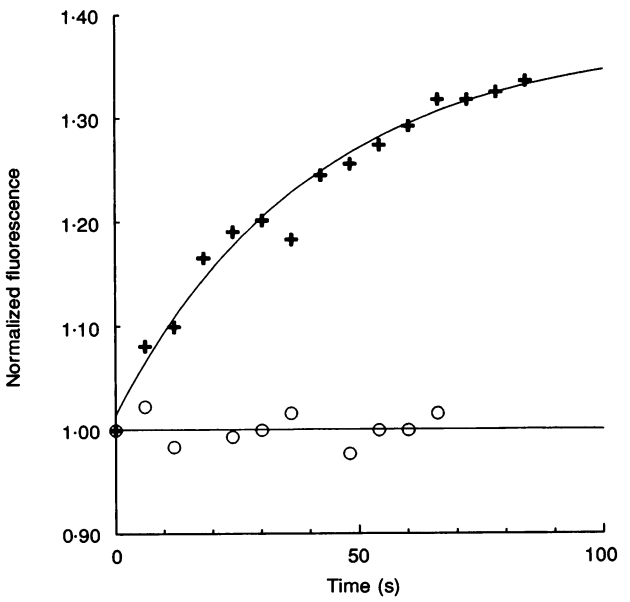

Figure 8. A venular capillary, transiently tight to rhodamine–albumin, even whilst leaky to Lucifer Yellow

Double occlusion (○) and single occlusion (+) on the same microvessel less than 2 min later. The curves are best fit regression and mono-exponential respectively. The initial rate of increase in rhodamine–albumin concentration in the single occlusion was used to calculate the volume flux.

observation that dye escaping from leaky microvessels did not accumulate in the perivascular interstitium, but appeared to be washed away immediately by the superfusing solution.

It is conceivable that the act of occlusion may damage the endothelium or release inflammatory mediators, but since similarly sized microvessels are occluded frequently in life, we think that it is a benign procedure. We have made permeability maps of occluded microvessels (Easton & Fraser, 1992*b*) and only rarely was there a significant increase in permeability in the region of occlusion, and when this did occur it was confined to within 10 μm of the site of occlusion (Easton, 1993).

The effect of convection on permeability

The idea that volume flow across a permeable membrane is an important consideration for large-molecule transport was confirmed by the paired double- and single-occlusion experiments. We found that restoration of capillary hydrostatic pressure has little effect on P'_{LY}, but reduces $P'_{Rh\text{-}A}$ to about half the double occlusion value. Figure 2 indicates that these hydrostatic pressure effects are sensitive to slit width for both the Lucifer Yellow and the albumin measurements and are consistent with the permeable pathway being formed by parallel-sided slits with a width between 20 and 25 nm.

The theoretical P'/P_0 for Lucifer Yellow can be calculated from the Péclet number and the estimate of σ by rearrangement of eqn (4) to

$$\frac{P'}{P_0} = Z - \frac{\mathrm{Pe}\sigma}{1-\sigma}. \quad (6)$$

This was found to be $P'/P_0 = 0{\cdot}92 \pm 0{\cdot}017$, which is satisfyingly close to the experimental value of $0{\cdot}94 \pm 0{\cdot}015$ (see Fig. 4) from different microvessels.

Variations in permeability to albumin

Permeability to rhodamine–albumin and Lucifer Yellow was measured in the same vessel at similar times when P_{LY} was of the order of 10^{-5} to 10^{-4} cm s^{-1}. Sometimes $P_{Rh\text{-}A}$ was consistent with unrestricted diffusion since $P_{LY}/P_{Rh\text{-}A}$ was similar to the ratio of their free diffusion coefficients, but often $P_{Rh\text{-}A}$ was below that expected from unrestricted diffusion and frequently too small to measure.

It has been pointed out to us that the variation in $P_{Rh\text{-}A}$ may be due to small residual pressures within the doubly occluded segment and not to any obstructing material. Fraser & Dallas (1993) provided evidence that the pathway across leaky cerebral microvessels is no more than 30 nm wide. Given this, examination of Fig. 2 shows that these hypothetical residual pressures would have to be unacceptably high (about 30 cmH_2O) to generate a sufficient volume flux to reduce $P'/P_{0,Rh\text{-}A}$ to zero. Thus the probable reason for the present results is a hindrance to the movement of albumin and whatever underlies the restriction to albumin can change with time in an apparently erratic fashion without having a large effect on the passage of Lucifer Yellow.

Cell surface GAGs have been put forward as a physiological mechanism by which the microvessel selectively restricts the movement of serum proteins across the vessel (Curry & Michel, 1980). There is little need for GAGs to perform this function in intact blood–brain barrier microvessels, and it is not known whether albumin is restricted in the disrupted blood–brain barrier. GAGs stained by cationized ferritin have been found on the luminal surface of retinal microvessels (Fitzgerald & Caldwell, 1990), but were absent from continuous cerebral microvessels (Schmidley & Wissig, 1986). It is possible that the process underlying the disruption of the blood–brain barrier also results in the triggering of the secretion of normally absent GAGs. If freshly secreted GAGs were sporadically shed into the passing blood it could account for our results, and would be similar to the heat-inflamed frog mesenteric microvessels described by Clough, Michel & Phillips (1988).

The present results are also consistent with several studies that model brain injury and the associated development of cerebral oedema (such as middle cerebral artery occlusion). These show that there is an early rise in permeability to albumin, which subsequently decreases and increases (Kuroiwa, Cahn, Juhler, Goping, Campbell & Klatzo, 1985*a*; Kuroiwa, Ting, Martinez & Klatzo, 1985*b*). Moreover, in these models the permeability to small molecules remains high despite a fall in albumin permeability (Kuroiwa *et al.* 1985*b*; Gotoh, Asano, Koide & Takakura, 1985) which is also consistent with our observations.

Route taken by Lucifer Yellow and rhodamine–albumin

Fraser & Dallas (1993) found that, in frog single pial microvessels disrupted by osmotic shock and trauma, the distribution of dye along the length of a disrupted vessel varied with different perfusion pressures in a way consistent with 22 nm slits. Similarly, Robinson & Rapoport (1987) showed that the disrupted barrier in rats was best described by a slit width of 22 nm. Clough & Michel (1988) independently measured the mean cleft width as 22 nm in frog mesenteric microvessels, but recently Neal & Michel (1992) have presented evidence for 0·5 μm diameter transcellular gaps, close to or sometimes including the junctions between cells, in inflamed mesenteric microvessels. Holes of a similar size and location were seen by Lossinsky, Pluta, Song, Badmajew, Moretz & Wisniewski (1991) in brain microvessels inflamed as a result of chronic relapsing experimental allergic encephalomyelitis.

The measured changes in permeability to Lucifer Yellow and rhodamine–albumin with changes in hydrostatic pressure in the present experiments were such that it is unlikely that the equivalent width of the open permeable pathway is greater than 25 nm. Thus the presence of 0·5 μm gaps seems improbable as they would give rise to large volume fluxes (200 times higher than the 22 nm wide slit of the same surface area) which would have lead to very low values of P'_{LY} (see Fig. 2). If the peri-junctional gaps were present, they must have been covered by some obstructing

material at all times, and GAGs of fibre radius 0·6 nm and void volume 0·95 would reduce the hydraulic conductance (and hence volume flow for a given pressure) to about 0·16 % of the value for a naked gap, and would reduce P_{LY} by about 60 %. This is consistent with the measurements of Neal & Clough (1992) who found that the hydraulic conductance increased in proportion to the total measured surface area of open endothelium and independently of the diameter of the gaps. GAGs of this nature would also be expected to reduce $P_{Rh\text{-}A}$ to about 1 % of its unhindered value, but there were many occasions when albumin behaved as if it were passing as freely as Lucifer Yellow with little hindrance by GAGs. Thus the fluctuation in hindrance is unlikely to be due to peri-junctional gaps occasionally shedding GAGs, since the volume flow through these periodically naked 0·5 μm passages would have been detected as occasional large falls in P'_{LY}. It seems that, if the peri-junctional gaps were present in these experiments, their contribution to permeability was in addition to that provided by open 22 nm slits. This raises the intriguing possibility that the peri-junctional gaps are the sites at which GAGs are secreted.

In summary, the pial venular capillaries, which normally have blood–brain barrier properties, become leaky on exposure. The nature of this leakiness is consistent with an open pathway 22 nm wide which is often completely open, but is sometimes obstructed by a material that restricts the passage of proteins. It is possible that this material is glycosaminoglycan secreted and shed by the endothelium.

APPENDIX

Estimate of hydrostatic pressure in a doubly occluded segment

If the doubly occluded microvessel is considered as a leaky elastic cylinder of length l, radius r, filtration coefficient L_p and compliance $\Delta V/\Delta P$, then as fluid leaves the segment across the endothelium the rate of pressure change will be

$$\frac{dP}{dt} = -J_v \frac{\Delta P}{\Delta V} \quad \text{(A1)}$$

and

$$P_t = P_0 \exp\left(-L_p A \frac{\Delta P}{\Delta V} t\right), \quad \text{(A2)}$$

with P_0 representing initial pressure, t time and A surface area. Smaje, Fraser & Clough (1980) showed that the compliance of mammalian mesenteric capillaries and venular capillaries could be calculated from estimates of vessel radius change in response to the small (*ca* 4 cmH_2O) transient changes in hydrostatic pressure which resulted from the heart beat. The compliance was such that the mean radius change was $\Delta r = \Delta P r^2/0{\cdot}726$ (units in cmH_2O, cm and s). Since $\Delta V = \pi l((r+\Delta r)^2 - r^2) \approx 2\pi r \Delta r l$ (for small Δr), $\Delta V/\Delta P = 2\pi l r^3/0{\cdot}726$. Thus for $l = 150$ and $r = 11$ μm (the approximate mean values in the present experiments) $\Delta V/\Delta P = 1{\cdot}73 \times 10^{-10}$ $cm^3\ cmH_2O^{-1}$. The filtration coefficient, L_p, was calculated from $L_p = P_{LY} w^2/D_{LY} 3\mu$ (w is the slit half-width, and μ viscosity of water) to be about 416×10^{-9} cm $cmH_2O^{-1}\ s^{-1}$ for open 22 nm wide slits ($P_{LY} = 31{\cdot}6 \times 10^{-6}$ cm s^{-1}), and the surface area of a doubly occluded microvascular segment $A = 2\pi r l = 3{\cdot}3 \times 10^{-5}$ cm^2. The time constant in eqn (A2) is thus about 0·064 s^{-1}, so that after 1 min the pressure within the segment would have fallen to about 1/40 of its peak value on occlusion. Alternatively, at the limit at which albumin was impermeable, presumably due to the presence of GAGs, the calculated L_p would be about 164×10^{-9} cm $cmH_2O^{-1}\ s^{-1}$ and the time constant 0·031 s^{-1}, so that the pressure would have fallen to about 1/6 of its value on occlusion.

REFERENCES

Bjerner, B., Broman, T. & Swensson, Å. (1944). Tierexperimentelle Untersuchungen über Schädigungen der Gefässe mit Permeabilitäts-storungen und Blutungen im Gehirm bei Insulin-, Cardiazol- und Elektroschoeckbehandlung. *Acta Psychiatrica et Neurologica Scandinavica* **19**, 431–452.

Butt, A. M., Jones, H. C. & Abbott, N. J. (1990). Electrical resistance across the blood–brain barrier in anaesthetized rats: a developmental study. *Journal of Physiology* **429**, 47–62.

Byrom, F. B. (1954). The pathogenesis of hypertensive encephalopathy and its relation to the malignant phase of hypertension. Experimental evidence from the hypertensive rat. *Lancet* ii, 201–211.

Clemedson, C. J., Hartelius, H. & Holmberg, G. (1958). The influence of carbon dioxide inhalation on the cerebral vascular permeability to trypan blue (the blood–brain barrier). *Acta Pathologica et Microbiologica Scandinavica* **42**, 137–149.

Clemente, C. P. & Holst, E. A. (1954). Pathological changes in neurons, neuroglia, and blood–brain barrier induced by X-irradiation of heads of monkeys. *Archives of Neurology and Psychiatry* **71**, 66–79.

Clough, G. & Michel, C. C. (1988). Quantitative comparisons of hydraulic conductivity and endothelial intercellular cleft dimensions in single frog capillaries. *Journal of Physiology* **405**, 563–576.

Clough, G., Michel, C. C. & Phillips, M. E. (1988). Inflammatory changes in permeability and ultrastructure of single vessels in the frog mesenteric microcirculation. *Journal of Physiology* **395**, 99–114.

Curry, F. E. (1974). A hydrodynamic description of the osmotic reflection coefficient with application to pore theory of transcapillary exchange. *Microvascular Research* **8**, 236–252.

Curry, F. E. (1984). Mechanics and thermodynamics of transcapillary exchange. In *Handbook of Physiology*, section 2, vol. IV, *Microcirculation*, chap. 8, ed. Renkin, E. M. & Michel, C. C., pp. 309–354. American Physiological Society, Washington.

Curry, F. E. & Huxley, V. H. (1982). Comparison of the capillary membrane properties determining fluid exchange in single capillaries and whole organs. *International Journal of Microcirculation: Clinical and Experimental* **1**, 381–391.

Curry, F. E., Joyner, W. L. & Rutledge, J. C. (1990). Graded modulation of frog microvessel permeability to albumin using ionophore A23187. *American Journal of Physiology* **258**, H587–598.

Curry, F. E. & Michel, C. C. (1980). A fiber matrix model of capillary permeability. *Microvascular Research* **20**, 96–99.

Easton, A. S. (1993). The characteristics of blood–brain barrier disruption studied in single microvessels *in vivo*. PhD Thesis, University of London.

Easton, A. S. & Fraser, P. A. (1991). Changes in permeability to large and small molecules in the disrupted blood–brain barrier. *International Journal of Microcirculation: Clinical and Experimental* **10**, 392.

EASTON, A. S. & FRASER, P. A. (1992*a*). Two phases of blood–brain barrier disruption in single cerebral microvessels of the anaesthetized rat. *Journal of Physiology* **446**, 503*P*.

EASTON A. S. & FRASER P. A. (1992*b*). Local changes in permeability within single cerebral venules of the anaesthetized rat. *International Journal of Microcirculation: Clinical and Experimental* **11**, 452.

EDVINSSON, L. & WEST, K. A. (1972). Experimental cerebral heat lesions produced by trephine craniotomy in rabbits. *Acta Pathologica et Microbiologica Scandinavica* (A), **80**, 134–138.

FITZGERALD, M. E. C. & CALDWELL, R. B. (1990). The retinal microvasculature of spontaneously diabetic BB rats: structure and luminal surface properties. *Microvascular Research* **39**, 15–27.

FRASER, P. A. & DALLAS, A. D. (1990). Measurement of filtration coefficient in single cerebral microvessels of the frog. *Journal of Physiology* **423**, 343–361.

FRASER, P. A. & DALLAS, A. D. (1993). Permeability of disrupted cerebral microvessels in the frog. *Journal of Physiology* **461**, 619–632.

GOTOH, O., ASANO, T., KOIDE, T. & TAKAKURA, K. (1985). Ischemic brain edema following occlusion of the middle cerebral artery in the rat: I. The time courses of the brain water, sodium and potassium contents and blood–brain barrier permeability to ^{125}I-albumin. *Stroke* **16**, 101–109.

JOHANSSON, B. B., LI, C.-L., OLSSON, Y. & KLATZO, I. (1970). The effect of acute arterial hypertension on the blood–brain barrier to protein tracers. *Acta Neuropathologica* **16**, 117–124.

KUROIWA, T., CAHN, R., JUHLER, M., GOPING, G., CAMPBELL, G. & KLATZO, I. (1985*a*). Role of extracellular proteins in the dynamics of vasogenic brain edema. *Acta Neuropathologica* **66**, 3–11.

KUROIWA, T., TING, P., MARTINEZ, H. & KLATZO, I. (1985*b*). The biphasic opening of the blood–brain barrier to proteins following temporary middle cerebral artery occlusion. *Acta Neuropathologica* **68**, 122–129.

LEVICK, J. R. (1987). Flow through interstitium and other fibrous matrices. *Quarterly Journal of Experimental Physiology* **72**, 409–438.

LOSSINSKY, A. S., PLUTA, R., SONG, M. J., BADMAJEW, V., MORETZ, R. C. & WISNIEWSKI, H. M. (1991). Mechanisms of inflammatory cell attachment in chronic relapsing experimental allergic encephalomyelitis: a scanning and high-voltage electron microscopic study of the injured mouse blood–brain barrier. *Microvascular Research* **41**, 299–310.

NEAL, C. R. & CLOUGH, G. (1992). The changes in hydraulic permeability and porous area of walls of mesenteric microvessels of pithed frogs during acute inflammation. *Journal of Physiology* **452**, 7*P*.

NEAL, C. R. & MICHEL, C. C. (1992). Transcellular openings through microvascular walls in acutely inflamed frog mesentery. *Experimental Physiology* **77**, 917–920.

RAPOPORT, S. I. (1970). Effect of concentrated solutions on blood–brain barrier. *American Journal of Physiology* **219**, 270–274.

ROBINSON, P. J. & RAPOPORT, S. I. (1987). Size selectivity of blood–brain barrier permeability at various times after osmotic opening. *American Journal of Physiology* **253**, R459–466.

SCHMIDLEY, J. W. & WISSIG, S. L. (1986). Basement membrane of central nervous system capillaries lacks Ruthenium Red-staining sites. *Microvascular Research* **32**, 300–314.

SMAJE, L. H., FRASER, P. A. & CLOUGH, G. (1980). The distensibility of single capillaries and venules in the cat mesentery. *Microvascular Research* **20**, 358–370.

TAMURA, A., GRAHAM, D. I., MCCULLOCH, J. & TEASDALE, G. M. (1981). Focal cerebral ischaemia in the rat: I. Description of technique and early neuropathological consequences following middle cerebral artery occlusion. *Journal of Cerebral Blood Flow and Metabolism* **1**, 53–60.

Acknowledgements

A.S.E. was supported by an MRC–Pfizer collaborative studentship.

Received 20 January 1993; accepted 26 July 1993.